Annals of Epidemiology 37 (2019) 51–56

Contents lists available at ScienceDirect

Annals of Epidemiology

Original article

The respiratory microbiota: associations with influenza symptomatology and viral shedding

Kyu Han Lee, PhD [a, b], Betsy Foxman, PhD [a], Guillermina Kuan, MD [c, d], Roger López, MSc [e], Kerby Shedden, PhD [f, g], Sophia Ng, PhD [h], Angel Balmaseda, MD [d, e], Aubree Gordon, PhD [h, *]

[a] Center for Molecular and Clinical Epidemiology of Infectious Diseases, Department of Epidemiology, School of Public Health, University of Michigan, Ann Arbor
[b] Department of Epidemiology, Bloomberg School of Public Health, Johns Hopkins University, Baltimore, MD
[c] Centro de Salud Sócrates Flores Vivas, Ministry of Health, Managua, Nicaragua
[d] Sustainable Sciences Institute, Managua, Nicaragua
[e] National Virology Laboratory, Centro Nacional de Diagnóstico y Referencia, Ministry of Health, Managua, Nicaragua
[f] Department of Statistics, University of Michigan, Ann Arbor
[g] Department of Biostatistics, School of Public Health, University of Michigan, Ann Arbor
[h] Department of Epidemiology, School of Public Health, University of Michigan, Ann Arbor

ARTICLE INFO

Article history:
Received 17 January 2019
Accepted 24 July 2019
Available online 31 July 2019

Keywords:
Influenza
Microbiota
Signs and symptoms
Virus shedding

ABSTRACT

Purpose: Manifestations of infection and the degree of influenza virus vary. We hypothesized that the nose/throat microbiota modifies the duration of influenza symptoms and viral shedding. Exploring these relationships may help identify additional methods for reducing influenza severity and transmission.
Methods: Using a household transmission study in Nicaragua, we identified secondary cases of influenza virus infection, defined as contacts with detectable virus or a greater than 4-fold change in hemagglutinin inhibition antibody titer. We characterized the nose/throat microbiota of secondary cases before infection and explored whether the duration of symptoms and shedding differed by bacterial community characteristics.
Results: Among 124 secondary cases of influenza, higher bacterial community diversity before infection was associated with longer shedding duration (Shannon acceleration factor [AF]: 1.61, 95% confidence interval [CI]: 1.24, 2.10) and earlier time to infection (Shannon AF: 0.72, 95% CI: 0.53, 0.97; Chao1 AF: 0.992, 95% CI: 0.986, 0.998). *Neisseria* and multiple other oligotypes were significantly associated with symptom and shedding durations and time to infection.
Conclusions: The nose/throat microbiota before influenza virus infection was associated with influenza symptoms and shedding durations. Further studies are needed to determine if the nose/throat microbiota is a viable target for reducing influenza symptoms and transmission.

Introduction

Clinical presentation of influenza virus infection can range from mild to severe [1]. Among the estimated 90 million new cases of influenza that occurred in young children in 2008, 20 million had acute lower respiratory infections, 1 million had severe acute respiratory lower infections, and 28,000–111,500 cases resulted in death [2]. Infectiousness, estimated by viral shedding, is not highly correlated with symptoms: viral shedding can be detected in asymptomatic cases but is often undetected in symptomatic cases [3–6]. A meta-analysis of challenge studies estimated that young adults shed for an average duration of 5 days after inoculation [3]. However, longer durations of shedding have been observed in more symptomatic cases [7] and in young children [4,8].

This heterogeneity in influenza illness and infectiousness has been largely attributed to the host immune response, which impacts pathogenicity and viral replication [9]. As the role of microbiota in stimulating host immunity has become evident [10–13],

* Corresponding author. Department of Epidemiology, School of Public Health, University of Michigan, 1415 Washington Heights, Ann Arbor, MI, 48109. Tel.: +1 734-763-3580; fax: +1 734-764-3192.
E-mail address: gordonal@umich.edu (A. Gordon).

https://doi.org/10.1016/j.annepidem.2019.07.013
1047-2797/

there have been increasing numbers of studies demonstrating associations between the microbiome and risk and severity of infectious diseases [14–16]. However, to our knowledge, no epidemiologic study has examined whether the microbiota is associated with symptoms or viral shedding during influenza virus infection. Identifying these links would lay the groundwork for developing symbiotic approaches to reduce influenza severity and transmission. This study fills this gap using data from a household transmission study in Nicaragua.

Materials and methods

Study population

This analysis uses data and samples collected by the Nicaraguan Household Transmission Study conducted in Managua, Nicaragua, between 2012 and 2014. Household index cases of influenza virus infection were identified at a primary health care center using the following ecriteria: 1) a positive QuickVue Influenza A + B rapid diagnostic test, 2) symptom onset of febrile acute respiratory illness (FARI; fever or feverishness with a rhinorrhea, sore throat, and/or cough) within the past 48 hours, 3) residing in a household with at least one other member (household contact), and 4) no household contacts with influenza symptoms in the two weeks before symptom onset in the index case.

Index cases and household contacts were invited to participate and monitored through up to 5 home visits, conducted at 2- to 3-day intervals. Nasal and oropharyngeal swabs were collected and combined at each visit. Blood samples were collected at enrollment and 30–45 days later. A secondary case was defined as a household contact with a positive real-time reverse transcription polymerase chain reaction (RT-PCR) result or a greater than or equal to 4-fold change in hemagglutination inhibition (HAI) antibody titers specific to the subtype/type identified in the index case.

A written informed consent or proxy consent was obtained for all participants. Verbal assent was obtained from children aged 5 years or older. The study was approved by the Institutional Review Boards at the University of Michigan and the Nicaraguan Ministry of Health.

Laboratory assays

Influenza type/subtype–specific RT-PCR was conducted on all samples using validated Centers for Disease Control and Prevention protocols [17]. Influenza type/subtype–specific HAI titers were measured using the validated World Health Organization protocols [18].

Microbiota characterization

Detailed methods used for microbiota characterization are discussed in Lee et al. [19]. Briefly, DNA was extracted from the first and last nasal/oropharyngeal sample collected from all index cases and household contacts. The V4 hypervariable region of the 16S rRNA gene was amplified and sequenced on an Illumina MiSeq System using a validated dual-indexing method [20]. Following alignment and quality filtering in mothur v1.38.1 [21] and oligotyping to assign reads to taxonomic units [22], Dirichlet multinomial mixture models [23] were used to assign all nasal/oropharyngeal samples to 5 bacterial community types (CTs) (Fig. S1). Each CT represents a group of samples with similar taxa compositions. We determined the number of CTs by estimating the Laplace approximation of the negative log models and identifying the point at which an increase in Dirichlet components resulted in minor reductions in model fit (Fig. S2). Considerations were placed on statistical power in downstream analyses. Taxonomy was assigned using the Human Oral Microbiome Database v14.51 [24] and blastn v2.2.23 [25].

Comparisons between CTs were conducted using all available microbiota data from all index cases and household contacts ($n = 1405$ samples). β-diversity, representing within-group dissimilarity of samples, was estimated using Bray-Curtis dissimilarity and Jaccard distance. α-diversity, representing within-sample community diversity, was estimated using the Shannon diversity index and Chao1 index. Shannon diversity accounts for both richness and evenness of taxa, whereas Chao1 only accounts for richness.

Influenza shedding and symptom data

Household contacts with 1 or more positive RT-PCR results during follow-up were defined as secondary cases with viral shedding. Shedding duration was estimated as the time between the first positive RT-PCR result and a negative RT-PCR result.

Study participants completed a daily symptom diary documenting the presence of the following symptoms: fever or feverishness, rhinorrhea, sore throat, and cough. To reduce potential bias from symptoms unrelated to influenza virus infection, we defined an influenza-associated illness period for each participant using symptom onset and alleviation dates. Illness onset was defined as the earliest date of any symptom. However, symptoms were excluded if they were alleviated >1 day before onset of viral shedding. Illness alleviation was defined as the date on which all symptoms were alleviated. Any recurring symptoms were excluded if the symptom recurred on 3 or after 3 days post viral shedding cessation or if fever recurred on 3 or after 3 days post fever alleviation. The duration of each symptom was estimated within the defined illness period. FARI was defined as the presence of fever plus rhinorrhea, sore throat, and/or cough and influenza-like illness was defined as fever plus sore throat and/or cough.

Statistical analysis

Accelerated failure time models using a generalized estimating equation approach were used to examine the relationship between bacterial community diversity and symptom duration, viral shedding duration, the serial interval, and time to shedding onset. Time to shedding onset was relative to symptom onset dates of index cases. Survival time was parameterized as a Weibull distribution in all models [26].

Models were repeated using CTs. We further explored whether outcomes were associated with the relative abundance of the 15 oligotypes that contributed to more than 50% of the difference between CTs. We ran single-oligotype models using $\log_{10}$-transformed relative abundance in consideration of the constant sum constraint [27] and the Benjamin-Hochberg method to correct for multiple testing.

We adjusted for age and sex in models estimating viral shedding and symptom. We adjusted for age, a smoker in the household, sex, and household crowding in models estimating time to shedding onset and estimating the serial interval. All models were adjusted for clustering by household. A summary of our models is available in Table S1. All statistical analyses were conducted using R, version 3.4.2 [28].

Availability of data and materials

Raw sequence reads have been deposited in a NCBI Sequence Read Archive repository (accession number PRJNA482032). Data sets generated and analyzed during the current study are available in an open-access Deep Blue Data repository (https://deepblue.lib.umich.edu/data/concern/generic_works/sb3979224?locale=en). Certain individual participant data have been excluded because of identifiability concerns.

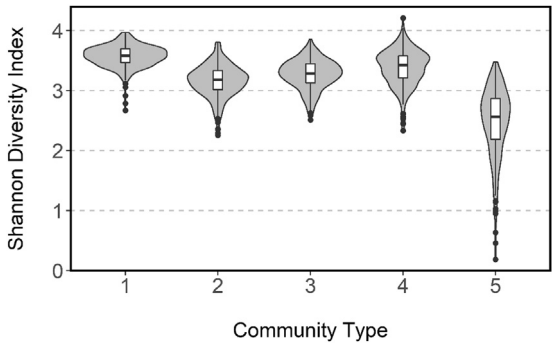

Fig. 1. Shannon diversity of bacterial community types based on the first and last nose/throat samples of 144 index cases and 573 household contacts from 144 households, Managua, Nicaragua, 2012–2014. Each violin plot contains a box plot with a kernel density estimation on either side depicting the distribution of data.

Results

Study population

A total of 144 index cases and 573 household contacts were enrolled in the Nicaraguan Household Transmission Study during 2012–2014. Following sequencing of the V4 region of the 16S rRNA of the first and last available nose/throat samples from all study participants, including both index cases and household contacts, and assignment to oligotypes, we used an unsupervised clustering technique to identify the 5 bacterial CTs (n = 1405 samples) (Figs. S1 and S2). CTs varied significantly in composition and structure as tested using permutational multivariate analysis of variance (beta diversity: Bray-Curtis dissimilarity, R^2 = 0.207, P = .001) and differed in alpha diversity (Shannon: Wilcoxon rank-sum, P < .001, Fig. 1; Chao1: Wilcoxon rank-sum, P < .001, Fig. S3). Most notably, CT 5 had the lowest alpha diversity. Clustering of samples into CTs was largely explained by a few oligotypes, with 50% of the difference between the single-CT and five-CT models attributed to 15 of the total 230 oligotypes. The relative abundance of these oligotypes is depicted in Figure 2. The complete taxa composition is available in Figure S4.

One hundred sixty secondary influenza virus infections were identified over a less than of equal to 13-day follow-up period using RT-PCR or a greater than or equal to 4-fold increase in HAI titer specific to the influenza type/subtype of the household index case 30–45 days after enrollment. Thirty-two were positive only by RT-PCR, 53 were positive only by HAI titer, and 62 were positive by both methods. Thirty-six household contacts with a positive RT-PCR result at the first home visit were excluded as nose/throat samples were not available before infection. Analysis was conducted on the remaining 124 secondary cases: 71 were positive for influenza by RT-PCR (57%) and 92 (74%) were positive by HAI during follow-up. Half of all secondary cases were adults (48%), and most infections were symptomatic (61%). Thirty-six secondary cases experienced FARI (29%), including 34 with influenza-like illness

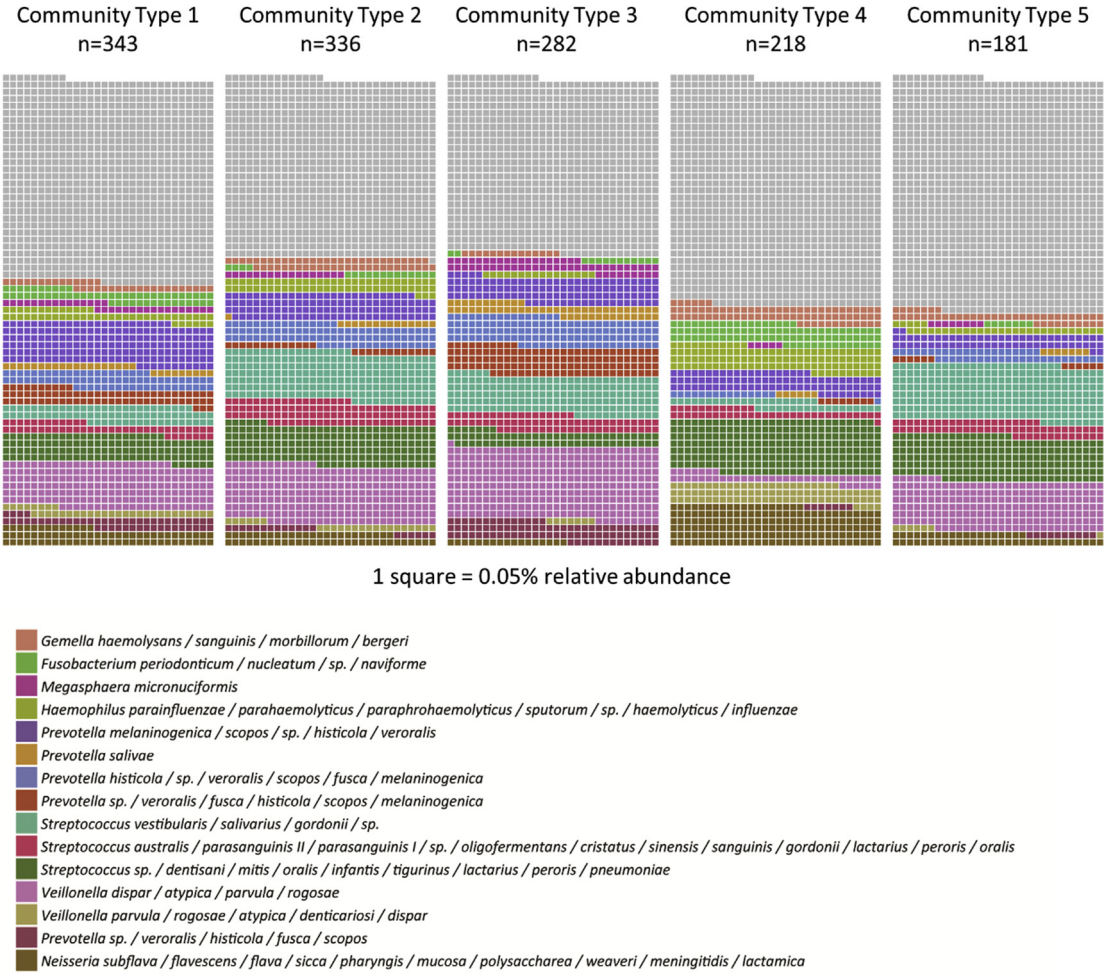

Fig. 2. Relative abundance of 15 oligotypes that contributed to 50% of difference between community types. Each square represents 0.05% relative abundance.

Table 1
Characteristics of 124 secondary influenza cases from 70 households, Managua, Nicaragua, 2012–2014, by bacterial community type

Characteristics	All ($n = 124$*)	Community type 1 ($n = 35$)	Community type 2 ($n = 31$)	Community type 3 ($n = 30$)	Community type 4 ($n = 14$)	Community type 5 ($n = 7$)
	No. (%)	No. (%)	No. (%)	No. (%)	No. (%)	No. (%)
Influenza type/subtype (RT-PCR)						
H1N1	12 (10)	2 (6)	3 (10)	2 (7)	4 (29)	0 (0)
H3N2	37 (30)	12 (34)	9 (29)	9 (30)	0 (0)	5 (71)
B	21 (17)	6 (17)	7 (23)	4 (13)	1 (7)	1 (14)
Co-infection	1 (1)	0 (0)	1 (3)	0 (0)	0 (0)	0 (0)
None	53 (43)	15 (43)	11 (35)	15 (50)	9 (64)	1 (14)
Influenza type/subtype (HAI)						
H1N1	18 (15)	4 (11)	5 (16)	4 (13)	4 (29)	0 (0)
H3N2	48 (39)	13 (43)	8 (26)	15 (50)	6 (43)	1 (0)
B	26 (21)	6 (17)	8 (26)	7 (23)	3 (21)	1 (14)
Co-infection	0 (0)	0 (0)	0 (0)	0 (0)	0 (0)	0 (0)
None	23 (19)	7 (20)	7 (23)	4 (13)	1 (7)	2 (29)
Missing	9 (7)	3 (9)	3 (10)	0 (0)	0 (0)	3 (43)
Age (y)						
0-5	19 (15)	5 (14)	6 (19)	1 (3)	0 (0)	5 (71)
6-17	45 (36)	16 (46)	10 (32)	13 (43)	4 (29)	1 (14)
≥18	60 (48)	14 (40)	15 (48)	16 (53)	10 (71)	1 (14)
Female	80 (65)	20 (57)	23 (74)	19 (63)	10 (71)	4 (57)
Influenza vaccination†	6 (5)	1 (3)	3 (10)	2 (7)	0 (0)	0 (0)
Smoker in household	59 (54)	16 (52)	14 (52)	17 (61)	6 (55)	4 (57)
Oseltamivir use	10 (8)	2 (6)	4 (13)	2 (7)	0 (0)	1 (14)
Symptoms						
Fever/feverishness	44 (35)	11 (31)	12 (39)	8 (27)	7 (50)	3 (43)
Rhinorrhea	53 (43)	14 (40)	16 (52)	10 (33)	7 (50)	3 (43)
Sore throat	35 (28)	8 (23)	12 (39)	6 (20)	5 (36)	2 (29)
Cough	60 (48)	14 (40)	18 (58)	14 (47)	9 (64)	3 (43)
FARI‡	36 (29)	7 (20)	11 (35)	6 (20)	6 (43)	3 (43)
ILI§	34 (27)	7 (20)	11 (35)	6 (20)	6 (43)	2 (29)

Secondary cases were defined as household contacts of index cases with a positive RT-PCR result for influenza or a greater than or equal to 4-fold change in HAI titer during follow-up.
FARI = febrile acute respiratory illness; HAI = hemagglutination inhibition; ILI = influenza-like illness; RT-PCR = reverse transcription polymerase chain reaction.
* Includes secondary cases with undefined community types.
† Before enrollment and in same year as index case.
‡ Fever/feverishness with rhinorrhea, sore throat, or cough.
§ Fever/feverishness with sore throat or cough.

(27%) (Table 1). Forty-one percent of households had more than 1 secondary case, suggesting clustering of secondary cases by household. Compared with persons with secondary infections without viral shedding ($n = 53$), persons with secondary infections with viral shedding ($n = 71$) were younger (mean: 16.7 years vs. 25.2 years, t-test, $P = .001$), more likely to be symptomatic (75% vs. 43% with 1 or more symptoms, χ^2 test, $P < .001$), and more likely to have FARI (42% vs. 6%, $\chi 2$ test, $P < .001$).

Bacterial community diversity before infection and symptom and shedding durations

We explored whether α-diversity before influenza virus infection was associated with symptom and shedding durations. We found no statistically significant associations between α-diversity and symptom durations (Table S2). Shannon diversity was positively associated with shedding duration (acceleration factor [AF]: 1.61; 95% confidence interval [CI]: 1.24, 2.10) (Fig. 3; Table S3). The mean predicted durations at the 25th and 75th quartiles of Shannon diversity (distribution among secondary cases) were 3.1 and 3.6 days, respectively.

Bacterial community diversity before infection and time to infection

We examined whether α-diversity was associated with time to infection using two different proxy measures, serial interval (defined as the time between onset of symptoms between an index case and a secondary case) and time to shedding onset, after adjusting for age, sex, a smoker in the household, household crowding, and clustering by household. The serial interval was negatively associated with Shannon diversity (AF: 0.72; 95% CI: 0.53, 0.97) and Chao1 (AF: 0.992; 95% CI: 0.986, 0.998). The mean serial interval was 3.7 and 3.2 days at the 25th and 75th quartiles of Shannon diversity, respectively, and 3.8 and 3.0 days at the 25th and 75th quartiles of Chao1, respectively. Chao1 was associated with earlier time to shedding onset (AF: 0.995; 95% CI: 0.990, 0.999). Mean serial interval was 5.8 and 5.3 days at the 25th and 75th quartiles of Chao1 index, respectively.

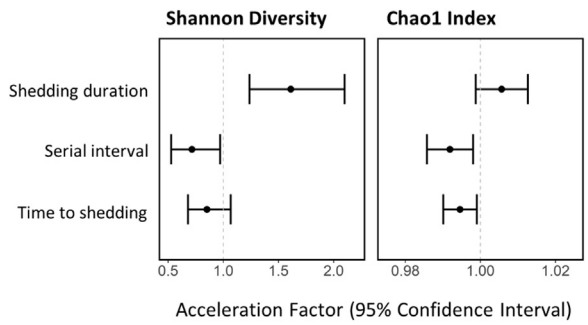

Fig. 3. Accelerated failure time models examining relationship between α-diversity and shedding duration, serial interval, and time to shedding onset among 124 secondary cases from 70 households, Managua, Nicaragua, 2012–2014. Models are not specific to influenza type/subtype.

Exploring CTs

We repeated our models using CTs as our primary exposure variable. Owing to small sample sizes of certain CTs, we also assessed whether our models were robust. We generated a bootstrapped data set with 100 iterations of randomly reassigned CTs and ran the viral shedding duration model for each iteration. The most uncommon CT was statistically significant in 26% of iterations suggesting an inflated type I error rate. All model results are included in Appendix for exploratory purposes and should be interpreted as such (Fig. S5).

The role of individual taxa

To explore the role of individual taxa, we examined whether the relative abundance of 15 oligotypes were associated with the duration of symptoms and viral shedding. We specifically focused on the oligotypes that contributed most to the difference between CTs (>50% of the difference) and used the Benjamin-Hochberg method to correct for multiple testing.

Duration of fever was negatively associated with *Veillonella parvula/rogosae/atypica/denticariosi/dispar* (AF: 0.66; 95% CI: 0.50, 0.86) (Table S4). Duration of runny nose was positively associated with *Neisseria* (AF: 1.41; 95% CI: 1.25, 1.60) and *Prevotella melaninogenica/scopos/*sp./*histicola/veroralis* (AF: 2.01; 95% CI: 1.46, 2.75). Duration of sore throat was positively associated with *Prevotella* sp./*veroralis/fusca/histicola/scopos/melaninogenica*, *Megasphaera micronuciformis*, and *Prevotella salivae*.

Shedding duration was positively associated with the abundance of *Fusobacterium* (AF: 1.14; 95% CI: 7%, 22%), *Neisseria* (AF: 1.16; 95% CI: 1.06, 1.27), and *Haemophilus* (AF: 1.13; 95% CI: 1.04, 1.23). Shedding duration was negatively associated with the abundance of *Streptococcus vestibularis/salivarius/gordonii*/sp. (AF: 0.61; 95% CI: 0.49, 0.77) and *Streptococcus australis/parasanguinis II/parasanguinis I*/sp./*oligofermentans/cristatus/sinensis/sanguinis/gordonii/lactarius/peroris/oralis* (AF: 0.59; 95% CI: 0.39, 0.91). *Fusobacterium* (AF: 0.89; 95% CI: 0.83, 0.95) and *Neisseria* (AF: 0.87; 95% CI: 0.79, 0.95) were associated with a shorter serial interval.

Sensitivity analysis

To investigate whether the criteria used to define illness periods affected our results, we reran our α-diversity models with three sets of modified criteria: 1) illness period does not exclude symptoms if fever recurs on 3 or after 3 days post fever alleviation; 2) illness period only considers influenza-like symptoms; and 3) all symptoms during follow-up contribute to illness period. Most model estimates remained the same or had minor differences that did not affect our overall conclusions (Table S5). The exception was in our serial interval models using criteria set 2 and 3, in which associations were no longer statistically significant. The direction of association did not change for Shannon diversity models, but the strength of the association was attenuated. For Chao1 models, the association shifted toward the null.

Discussion

We explored whether the nose/throat microbiota before influenza virus infection influenced the duration of symptoms, viral shedding, and time to infection among secondary influenza cases identified by RT-PCR or a greater than or equal to 4-fold increase in HAI titers. Community diversity before influenza virus infection was associated with viral shedding duration. Secondary cases with less diverse bacterial communities had a longer period of viral shedding and signs of infection were observed earlier.

Several oligotypes were associated with symptoms and shedding. Among them, a *Neisseria* oligotype was of particular interest as it was associated with multiple outcomes including earlier signs of infection (by serial interval and viral shedding), longer durations of symptoms, and longer viral shedding. There is little information regarding biological interactions between *Neisseria* and influenza. However, there is some evidence that the outer membrane vesicles of *Neisseria* can act as a mucosal adjuvant. Findings from intranasal influenza vaccine study demonstrated substantial increases in both IgG and IgA antibodies when inactivated *Neisseria meningitidis* was added as an adjuvant to the vaccine [29].

Our findings are consistent with results of murine experiments demonstrating a relationship between the gut microbiome and influenza symptoms and viral shedding. Mice treated with antibiotics before inoculation with influenza virus expressed enhanced disease severity and increased risk of death [13]. Among mice with microbiomes disrupted by antibiotics, macrophages expressed defective responses to type I and type II interferons (IFNs) [13] and exhibited defective T-cell and B-cell responses linked to reduced priming of inflammasome-dependent cytokines [11]. These impairments resulted in higher viral replication [11,13]. However, these studies did not characterize the microbiota using an untargeted 16S rRNA taxonomic screen, making it difficult to connect our epidemiologic findings with specific biological mechanisms.

Replication and exploration of the mechanisms underlying our results are needed to evaluate whether our observations are causal. A particular limitation of our study is we were unable to determine if the characteristics of nose/throat microbiota are risk factors or risk markers, that is, whether host factors leading to differences in clinical outcomes of influenza also lead to the observed nose/throat microbiota. Larger studies that oversample young children and assess immune response and animal models are needed to clarify the relationship. Moreover, a more comprehensive assessment of the microbiota (metagenomics and metabolomics) would enable evaluation of other microbiota characteristics beyond α-diversity and selected taxa.

Our study has several strengths. As a case-ascertained study, we were able to characterize the nose/throat microbiota of secondary cases a few days before infection. By using both RT-PCR and HAI, we were able to improve our detection of secondary cases. Finally, daily symptom diaries and regular RT-PCR testing over follow-up allowed us to estimate time-to-event outcomes related to influenza symptoms and viral shedding. However, there are also several potential limitations. Any criteria used to define an influenza-associated illness period are subject to misclassification. However, sensitivity analysis indicates our criteria did not meaningfully affect our results. Finally, our study does not consider the infectiousness of index cases in time to infection estimates and we were inadequately powered to examine influenza subtype–specific relationships.

Conclusions

In conclusion, our study identified associations between the duration of influenza symptoms, viral shedding, and the nose/throat bacterial microbiota before influenza infection. By extension, the microbiota may influence influenza transmission, which likely is dependent on both the duration and level of viral shedding and the presence of symptoms. Current methods for reducing influenza transmission and disease severity involve reducing exposure to the virus, vaccination, and antiviral treatment. However, complementary strategies should be explored to reduce the 3–5 million cases of severe illness [30] and 400,000 deaths [31] estimated to occur each year. The microbiome may provide opportunities for reducing this burden. Randomized controlled studies have shown drastic reductions in respiratory tract infections among newborns given

synbiotics, which are estimated to cost around $1 per person for 1 week of treatment [14,15]. Future studies should investigate causal pathways between the microbiome and respiratory infections and evaluate the impact of synbiotics in different populations.

Acknowledgment

This work was supported by NIH NIAID (grant no. R21 AI119463). Data collection was supported by NIH (grant no. U01 AI088654), the Fogarty International Center (grant no. K02 TW009483) and National Institutes of Health Department of Health and Human Services under the contract number HHSN272201400031C. Additional funding came from the Tinker Foundation, University of Michigan Center for Latin America and Caribbean Studies, University of Michigan International Institute, and University of Michigan Rackham Graduate School. The authors are grateful to the participants of the Nicaraguan Household Transmission Study and our collaborators at the Nicaraguan Ministry of Health and Sustainable Sciences Institute. The authors thank the University of Michigan Microbial Systems Laboratories for 16S rRNA sequencing. The authors also thank Dr. Marie Griffin for reviewing an earlier draft of this manuscript.

References

[1] Widdowson M-A, Monto AS. Epidemiology of influenza. In: Webster RG, Monto AS, Braciale TJ, Lamb RA, editors. Textb. Influenza. 2nd ed. Chichester, UK: Wiley; 2013.
[2] Nair H, Brooks WA, Katz M, Roca A, Berkley JA, Madhi SA, et al. Global burden of respiratory infections due to seasonal influenza in young children: a systematic review and meta-analysis. Lancet 2011;378:1917–30.
[3] Carrat F, Vergu E, Ferguson NM, Lemaitre M, Cauchemez S, Leach S, et al. Time lines of infection and disease in human influenza: a review of volunteer challenge studies. Am J Epidemiol 2008;167:775–85.
[4] Ng S, Lopez R, Kuan G, Gresh L, Balmaseda A, Harris E, et al. The timeline of influenza virus shedding in children and adults in a household transmission study of influenza in Managua, Nicaragua. Pediatr Infect Dis J 2016;35:583–6.
[5] Cowling BJ, Chan KH, Fang VJ, Lau LLH, So HC, Fung ROP, et al. Comparative epidemiology of pandemic and seasonal influenza A in households. N Engl J Med 2010;362:2175–84.
[6] Ferguson NM, Cummings DAT, Cauchemez S, Fraser C, Riley S, Meeyai A, et al. Strategies for containing an emerging influenza pandemic in Southeast Asia. Nature 2005;437:209.
[7] Ip DKM, Lau LLH, Leung NHL, Fang VJ, Chan K-H, Chu DKW, et al. Viral shedding and transmission potential of asymptomatic and paucisymptomatic influenza virus infections in the community. Clin Infect Dis 2017;64:736–42.
[8] Loeb M, Singh PK, Fox J, Russell ML, Pabbaraju K, Zarra D, et al. Longitudinal study of influenza molecular viral shedding in Hutterite communities. J Infect Dis 2012;206:1078–84.
[9] Hayden FG, de Jong MD. Human influenza: Pathogenesis, clinical features, and management. In: Webster RG, Monto AS, Braciale TJ, Lamb RA, editors. Textb. Influenza. 2nd ed. Chichester, UK: Wiley; 2013.
[10] Ivanov II, Atarashi K, Manel N, Brodie EL, Shima T, Karaoz U, et al. Induction of intestinal Th17 Cells by segmented filamentous bacteria. Cell 2009;139:485–98.
[11] Ichinohe T, Pang IK, Kumamoto Y, Peaper DR, Ho JH, Murray TS, et al. Microbiota regulates immune defense against respiratory tract influenza A virus infection. Proc Natl Acad Sci USA 2011;108:5354.
[12] Shaw MH, Kamada N, Kim Y-G, Núñez G. Microbiota-induced IL-1β, but not IL-6, is critical for the development of steady-state TH17 cells in the intestine. J Exp Med 2012;209:251–8.
[13] Abt MC, Osborne LC, Monticelli LA, Doering TA, Alenghat T, Sonnenberg GF, et al. Commensal bacteria calibrate the activation threshold of innate antiviral immunity. Immunity 2012;37:158–70.
[14] Panigrahi P, Parida S, Nanda NC, Satpathy R, Pradhan L, Chandel DS, et al. A randomized synbiotic trial to prevent sepsis among infants in rural India. Nature 2017;548:407–12.
[15] Luoto R, Ruuskanen O, Waris M, Kalliomäki M, Salminen S, Isolauri E. Prebiotic and probiotic supplementation prevents rhinovirus infections in preterm infants: A randomized, placebo-controlled trial. J Allergy Clin Immunol 2014;133:405–13.
[16] Schuijt TJ, Lankelma JM, Scicluna BP, de Sousa e Melo F, Roelofs JJTH, de Boer JD, et al. The gut microbiota plays a protective role in the host defence against pneumococcal pneumonia. Gut 2016;65:575–83.
[17] Novel Swine-Origin Influenza A (H1N1) Virus Investigation Team, Dawood FS, Jain S, Finelli L, Shaw MW, Lindstrom S, et al. Emergence of a novel swine-origin influenza A (H1N1) virus in humans. N Engl J Med 2009;360:2605–15.
[18] World Health Organization. WHO Manual on Animal Influenza Diagnosis and Surveillance. Geneva, Switzerland: World Health Organization; 2002.
[19] Lee KH, Gordon A, Shedden K, Kuan G, Ng S, Balmaseda A, et al. The respiratory microbiome and susceptibility to influenza virus infection. PLoS One 2019;14:e0207898.
[20] Kozich JJ, Westcott SL, Baxter NT, Highlander SK, Schloss PD. Development of a Dual-Index Sequencing Strategy and Curation Pipeline for Analyzing Amplicon Sequence Data on the MiSeq Illumina Sequencing Platform. Appl Environ Microbiol 2013;79:5112–20.
[21] Schloss PD, Westcott SL, Ryabin T, Hall JR, Hartmann M, Hollister EB, et al. Introducing mothur: open-source, platform-independent, community-supported software for describing and comparing microbial communities. Appl Environ Microbiol 2009;75:7537–41.
[22] Eren AM, Morrison HG, Lescault PJ, Reveillaud J, Vineis JH, Sogin ML. Minimum entropy decomposition: unsupervised oligotyping for sensitive partitioning of high-throughput marker gene sequences. ISME J 2015;9:968–79.
[23] Holmes I, Harris K, Quince C. Dirichlet multinomial mixtures: generative models for microbial metagenomics. PLoS One 2012;7:e30126.
[24] Chen T, Yu W-H, Izard J, Baranova OV, Lakshmanan A, Dewhirst FE. The Human Oral Microbiome Database: a web accessible resource for investigating oral microbe taxonomic and genomic information. Database 2010;2010:baq013.
[25] Altschul SF, Gish W, Miller W, Myers EW, Lipman DJ. Basic local alignment search tool. J Mol Biol 1990;215:403–10.
[26] Cowling BJ, Fang VJ, Riley S, Peiris JSM, Leung GM. Estimation of the serial interval of influenza. Epidemiol Camb Mass 2009;20:344–7.
[27] Aitchison J. The Statistical Analysis of Compositional Data. J R Stat Soc Ser B Methodol 1982;44:139–77.
[28] R Core Team. R. A language and environment for statistical computing. Vienna, Austria: R Foundation for Statistical Computing; 2017.
[29] Berstad AKH, Andersen SR, Dalseg R, Drømtorp S, Holst J, Namork E, et al. Inactivated meningococci and pertussis bacteria are immunogenic and act as mucosal adjuvants for a nasal inactivated influenza virus vaccine. Vaccine 2000;18:1910–9.
[30] World Health Organization. Influenza. Immun Vaccines Biol Influenza. http://www.who.int/immunization/topics/influenza/en/. [Accessed 17 February 2017].
[31] Iuliano AD, Roguski KM, Chang HH, Muscatello DJ, Palekar R, Tempia S, et al. Estimates of global seasonal influenza-associated respiratory mortality: a modelling study. Lancet 2017;391:1285–300.

Appendix

Table S1
Summary of accelerated failure time models used to investigate the relationship between the nose/throat microbiota and various symptom and viral shedding outcomes

Model	Community diversity	Age	Sex	Smoker in household	Crowding
Symptom duration	Yes	Yes	Yes	No	No
Shedding duration	Yes	Yes	Yes	No	No
Serial interval	Yes	Yes	Yes	Yes	Yes
Time to shedding onset	Yes	Yes	Yes	Yes	Yes

Models were additionally controlled for clustering by household and were not specific to influenza type/subtype. Community diversity, age, sex, smoker in household, and crowding are independent variables included in the model. Models were rerun using community types and $\log_{10}$-transformed relative abundance of 15 oligotypes that contributed to 50% of difference between community types.

Table S2
Accelerated failure time models estimating association between alpha diversity and symptom duration among 124 secondary cases from 70 households, Managua, Nicaragua, 2012–2014

Outcome	Shannon diversity	Chao1 index
	Acceleration factor (95% confidence interval)	
Duration of fever	0.80 (0.31, 2.07)	1.00 (0.99, 1.01)
Duration of runny nose	1.87 (0.67, 5.24)	1.01 (0.996, 1.03)
Duration of sore throat	1.01 (0.55, 1.85)	1.00 (0.99, 1.01)
Duration of cough	1.39 (0.56, 3.49)	1.00 (0.99, 1.02)

Table S3
Accelerated failure time models estimating the association between alpha diversity and shedding and time to infection among 124 secondary cases from 70 households, Managua, Nicaragua, 2012–2014

Model	Shedding duration	Serial interval	Time to shedding onset
	Acceleration factor (95% confidence interval)		
Shannon diversity	1.61 (1.24, 2.10)	0.72 (0.53, 0.97)	0.85 (0.68, 1.07)
<5 y	1.04 (0.64, 1.69)	0.72 (0.49, 1.05)	0.87 (0.62, 1.21)
6–17 y	0.95 (0.66, 1.37)	1.09 (0.76, 1.56)	0.98 (0.72, 1.31)
Female	1.06 (0.77, 1.47)	1.02 (0.73, 1.42)	0.92 (0.73, 1.15)
Smoker in household	—	0.95 (0.65, 1.47)	0.86 (0.62, 1.19)
Household crowding	—	0.93 (0.63, 1.38)	1.04 (0.77, 1.40)
Chao1 index	1.01 (0.999, 1.01)	0.99 (0.99, 0.998)	0.99 (0.99, 0.999)
<5 y	1.08 (0.60, 1.96)	0.66 (0.45, 0.95)	0.75 (0.51, 1.11)
6–17 y	0.98 (0.67, 1.43)	1.05 (0.74, 1.48)	0.91 (0.68, 1.21)
Female	1.09 (0.78, 1.52)	1.02 (0.73, 1.43)	0.89 (0.71, 1.12)
Smoker in household	—	0.95 (0.65, 1.47)	0.86 (0.64, 1.17)
Household crowding	—	0.93 (0.63, 1.38)	1.10 (0.80, 1.50)

Table S4
Single-oligotype models using $\log_{10}$-transformed relative abundance of 15 oligotypes that contributed to 50% of difference between community types among 124 secondary cases from 70 households, Managua, Nicaragua, 2012–2014

Oligotype	Fever duration		Runny nose duration	
	AF (95% CI)	q-value*	AF (95% CI)	q-value*
Veillonella 1	1.20 (0.82, 1.75)	0.409	1.27 (0.89, 1.81)	0.564
Streptococcus 1	1.34 (0.83, 2.17)	0.409	0.98 (0.49, 1.95)	0.945
Fusobacterium	0.89 (0.64, 1.23)	0.772	1.30 (1.09, 1.55)	0.020
Streptococcus 2	1.04 (0.51, 2.09)	0.912	0.40 (0.16, 1.03)	0.214
Prevotella 1	1.05 (0.89, 1.25)	0.730	0.97 (0.82, 1.15)	0.945
Gemella	0.64 (0.42, 0.99)	0.200	0.97 (0.47, 2.00)	0.945
Neisseria	0.85 (0.65, 1.11)	0.730	1.41 (1.25, 1.60)	<0.001
Haemophilus	0.64 (0.42, 0.98)	0.285	1.09 (0.42, 2.87)	0.945
Prevotella 2	1.12 (0.96, 1.31)	0.409	1.08 (0.83, 1.39)	0.874
Prevotella 3	1.23 (1.03, 1.48)	0.200	1.31 (0.92, 1.40)	0.625
Prevotella 4	1.10 (0.71, 1.70)	0.772	2.01 (1.46, 2.75)	<0.001
Streptococcus 3	1.22 (0.74, 2.01)	0.648	1.36 (0.46, 4.00)	0.874
Megasphaera	1.02 (0.91, 1.14)	0.772	1.06 (0.95, 1.18)	0.718
Prevotella 5	1.09 (0.91, 1.31)	0.648	1.01 (0.80, 1.28)	0.945
Veillonella 2	0.66 (0.50, 0.86)	0.030	0.88 (0.63, 1.25)	0.874
	Sore throat duration†		Cough duration	
Veillonella 1	0.95 (0.51, 1.79)	0.990	0.81 (0.47, 1.40)	0.759
Streptococcus 1	1.00 (0.58, 1.73)	0.990	0.69 (0.39, 1.22)	0.621
Fusobacterium	1.23 (0.96, 1.57)	0.291	1.33 (1.02, 1.72)	0.255
Streptococcus 2	1.30 (0.63, 2.70)	0.894	0.63 (0.28, 1.40)	0.621
Prevotella 1	0.99 (0.55, 1.78)	0.990	0.84 (0.64, 1.09)	0.621
Gemella	1.12 (0.62, 2.01)	0.976	0.85 (0.51, 1.42)	0.782
Neisseria	0.85 (0.60, 1.20)	0.774	1.37 (1.03, 1.82)	0.292
Haemophilus	1.52 (0.88, 2.65)	0.340	1.27 (0.78, 2.06)	0.694
Prevotella 2	1.17 (0.98, 1.39)	0.291	0.92 (0.73, 1.14)	0.759
Prevotella 3	1.27 (1.13, 1.42)	<0.001	1.06 (0.84, 1.33)	0.782
Prevotella 4	1.22 (0.60, 2.49)	0.963	1.42 (0.88, 2.29)	0.621
Streptococcus 3	1.11 (0.64, 1.92)	0.976	0.79 (0.35, 1.78)	0.782
Megasphaera	1.14 (1.04, 1.24)	0.020	0.98 (0.86, 1.13)	0.844
Prevotella 5	1.22 (1.07, 1.39)	0.015	0.97 (0.79, 1.19)	0.844
Veillonella 2	1.02 (0.72, 1.44)	0.990	0.83 (0.62, 1.12)	0.621

Oligotype	Shedding duration		Serial interval		Time to shedding onset	
	AF (95% CI)	q-value*	AF (95% CI)	q-value*	AF (95% CI)	q-value*
Veillonella 1	0.83 (0.67, 1.02)	0.171	1.31 (0.98, 1.74)	0.255	1.16 (0.89, 1.50)	0.528
Streptococcus 1	0.61 (0.49, 0.77)	<0.001	1.02 (0.74, 1.40)	0.920	0.88 (0.70, 1.12)	0.528
Fusobacterium	1.14 (1.06, 1.23)	0.002	0.89 (0.83, 0.95)	0.015	0.97 (0.93, 1.02)	0.528
Streptococcus 2	1.25 (0.85, 1.84)	0.353	1.07 (0.79, 1.44)	0.773	0.94 (0.61, 1.46)	0.845
Prevotella 1	0.86 (0.69, 1.07)	0.286	0.97 (0.79, 1.20)	0.840	0.97 (0.90, 1.04)	0.528
Gemella	1.16 (0.87, 1.55)	0.399	1.31 (0.91, 1.89)	0.362	1.23 (0.88, 1.71)	0.528
Neisseria	1.16 (1.06, 1.27)	0.009	0.87 (0.79, 0.95)	0.015	0.97 (0.90, 1.04)	0.598
Haemophilus	1.13 (1.04, 1.23)	0.023	0.93 (0.68, 1.26)	0.773	1.01 (0.96, 1.07)	0.772
Prevotella 2	1.05 (0.94, 1.17)	0.430	0.92 (0.83, 1.01)	0.255	0.93 (0.87, 1.00)	0.360
Prevotella 3	1.04 (0.90, 1.21)	0.570	1.07 (0.92, 1.25)	0.554	0.98 (0.91, 1.05)	0.693
Prevotella 4	1.21 (0.97, 1.52)	0.171	0.81 (0.63, 1.03)	0.384	0.90 (0.79, 1.03)	0.528
Streptococcus 3	0.59 (0.39, 0.91)	0.049	0.88 (0.66, 1.19)	0.255	0.84 (0.62, 1.13)	0.528
Megasphaera	0.97 (0.88, 1.06)	0.553	1.07 (0.96, 1.18)	0.409	0.99 (0.92, 1.07)	0.872
Prevotella 5	1.10 (0.99, 1.24)	0.171	0.94 (0.72, 1.22)	0.773	0.94 (0.89, 1.00)	0.360
Veillonella 2	1.10 (0.95, 1.27)	0.294	0.86 (0.66, 1.12)	0.435	0.97 (0.88, 1.06)	0.680

Oligotype	Full taxonomic classification
Veillonella 1	*Veillonella dispar/atypica/parvula/rogosae*
Streptococcus 1	*Streptococcus vestibularis/salivarius/gordonii*/sp.
Fusobacterium	*Fusobacterium periodonticum/nucleatum* subsp. *animalis*/sp./*nucleatum* subsp. *Vincentii/nucleatum* subsp. *polymorphum/naviforme/nucleatum* subsp. *nucleatum*
Streptococcus 2	*Streptococcus* sp./*dentisani/mitis/oralis/infantis/tigurinus/lactarius/peroris/pneumoniae*
Prevotella 1	*Prevotella histicola*/sp./*veroralis/scopos/fusca/melaninogenica*
Gemella	*Gemella haemolysans/sanguinis/morbillorum/bergeri*
Neisseria	*Neisseria subflava/flavescens/flava/sicca/pharynges/mucosa/polysaccharea/weaver/meningitidis/lactamica*
Haemophilus	*Haemophilus parainfluenzae/parahaemolyticuss/paraphrohaemolyticus/sputorum*/sp./*haemolyticus/influenzae*
Prevotella 2	*Prevotella* sp./*veroralis/histicola/fusca/scopos*
Prevotella 3	*Prevotella* sp./*veroralis/fusca/histicola/scopos/melaninogenica*
Prevotella 4	*Prevotella melaninogenica/scopos*/sp./*histicola/veroralis*
Streptococcus 3	*Streptococcus australis/parasanguinis II/parasanguinis I*/sp./*oligofermentans/cristatus/sinensis/sanguinis/gordonii/lactarius/peroris/oralis*
Megasphaera	*Megasphaera micronuciformis*
Prevotella 5	*Prevotella salivae*
Veillonella 2	*Veillonella parvula/rogosae/atypica/denticariosi/dispar*

Benjamin-Hochberg method to correct for multiple testing.
* Corrected for multiple testing using the Benjamin-Hochberg method.
† Children 0–5 years of age were removed from the sore throat model as they cannot reliably report the symptom.

Table S5
Sensitivity analysis using alternative definitions of illness period

Model	Original definition	Alternative 1	Alternative 2	Alternative 3
	Acceleration factor (95% confidence interval)			
Shannon diversity				
Fever	0.80 (0.31, 2.07)	0.59 (0.20, 1.76)	0.82 (0.32, 2.12)	0.52 (0.18, 1.52)
Runny nose	1.87 (0.67, 5.24)	1.87 (0.67, 5.24)	1.35 (0.64, 2.83)	1.44 (0.67, 3.09)
Sore throat	1.01 (0.55, 1.85)	1.01 (0.55, 1.85)	1.01 (0.55, 1.85)	1.00 (0.55, 1.83)
Cough	1.39 (0.56, 3.49)	1.39 (0.56, 3.49)	1.24 (0.52, 3.04)	1.30 (0.52, 3.27)
Serial interval	0.72 (0.53, 0.97)	0.72 (0.53, 0.97)	0.88 (0.67, 1.16)	0.92 (0.71, 1.21)
Chao1 index				
Fever	1.00 (0.99, 1.01)	0.99 (0.98, 1.01)	0.99 (0.99, 1.01)	0.99 (0.98, 1.01)
Runny nose	1.01 (0.996, 1.03)	1.01 (0.99, 1.03)	1.01 (0.996, 1.02)	1.01 (0.996, 1.02)
Sore throat	1.00 (0.99, 1.01)	1.00 (0.99, 1.01)	1.00 (0.99, 1.01)	1.01 (0.99, 1.02)
Cough	1.00 (0.99, 1.02)	1.00 (0.99, 1.02)	1.00 (0.99, 1.02)	1.00 (0.99, 1.01)
Serial interval	0.99 (0.99, 0.998)	0.99 (0.99, 0.998)	1.00 (0.99, 1.002)	1.00 (0.99, 1.01)

Alternative 1: The influenza-associated illness period does not exclude symptoms if fever recurs on 3 or after 3 days post fever alleviation. Alternative 2: The influenza-associated illness period only considers symptoms of influenza-like illness. Alternative 3: All symptoms of acute respiratory illness during follow-up contribute to the influenza-associated illness period.

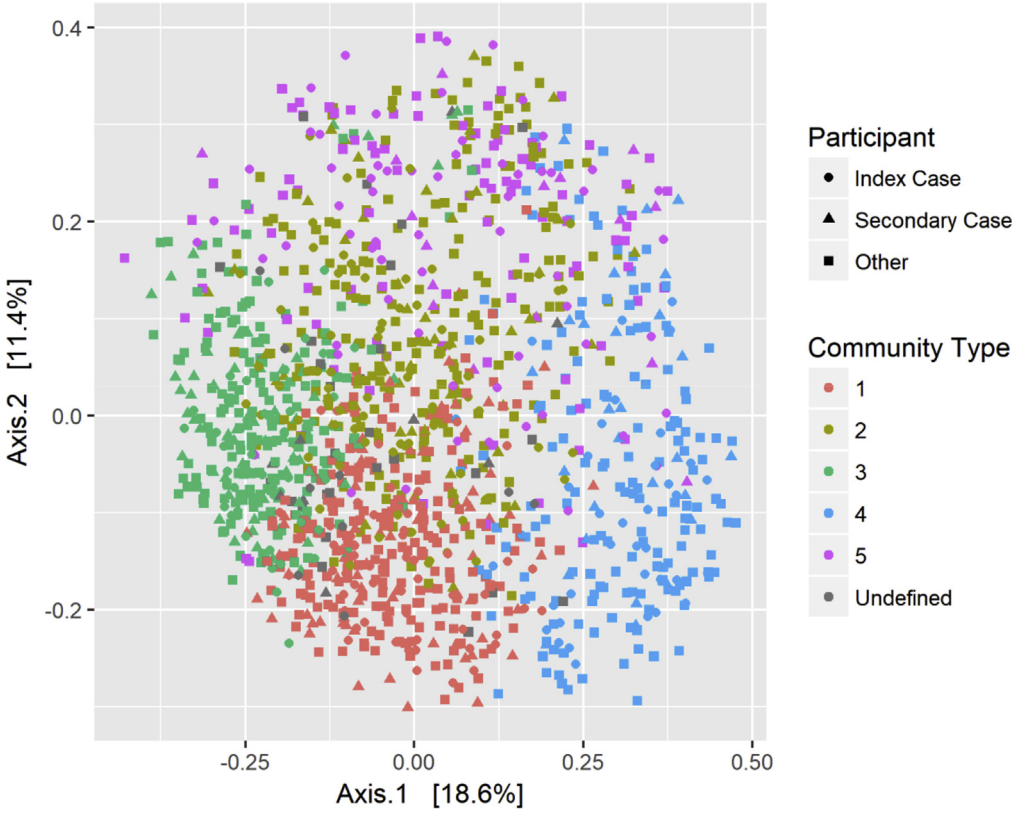

Fig. S1. Principal coordinates analysis of nose/throat samples assigned to community types. 1405 nose/throat samples from 717 study participants residing in 144 households in Managua, Nicaragua, 2012–2014. Based on Bray-Curtis dissimilarity.

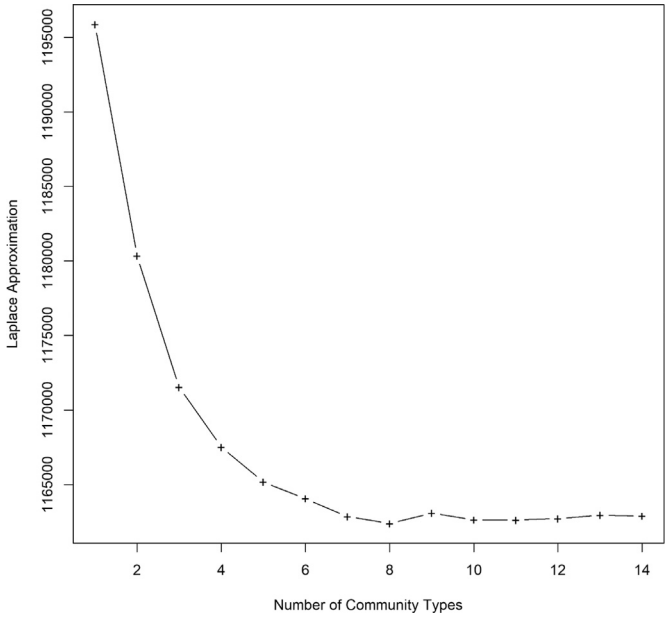

Fig. S2. Model fit of negative log models by number of Dirichlet components using the first and last samples of all study participants ($n = 1405$ samples). We determined the number of community types by estimating the Laplace approximation of the negative log models and identifying the point at which an increase in Dirichlet components resulted in minor reductions in model fit. Considerations were placed on statistical power in downstream analyses.

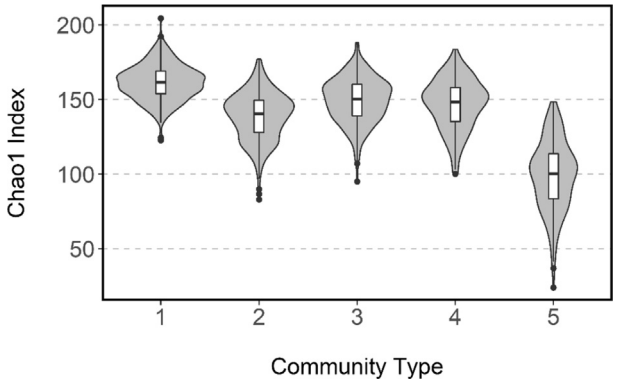

Fig. S3. Chao1 by community types based on the first and last nose/throat samples of 717 study participants from 144 households, Managua, Nicaragua, 2012–2014. Each violin plot contains a box plot with a kernel density estimation on each side depicting the distribution of data.

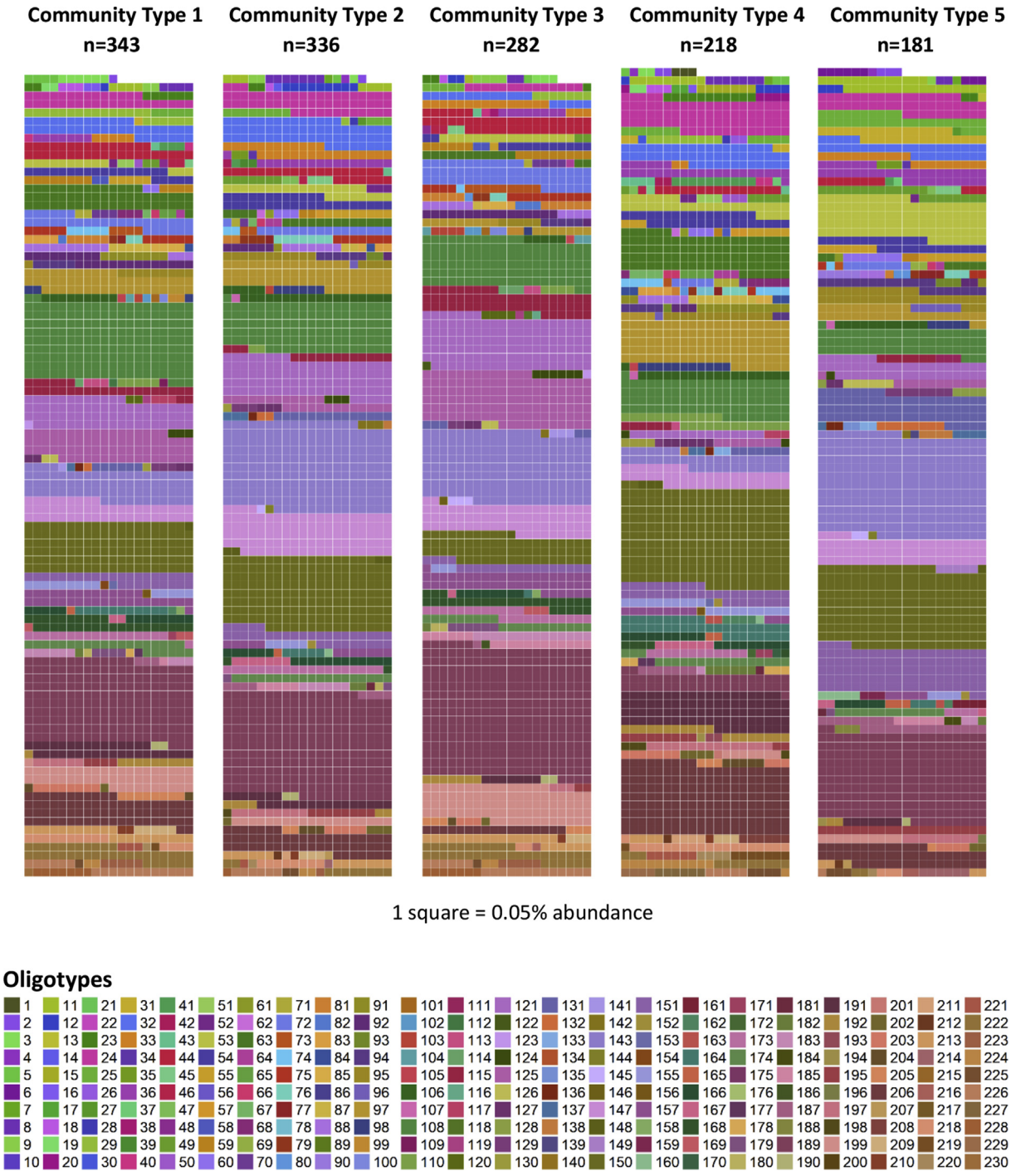

Fig. S4. Relative abundance of oligotypes by community type. Based on the first and last nose/throat samples of 717 study participants from 144 households, Managua, Nicaragua, 2012–2014. Each square represents 0.05% relative abundance.

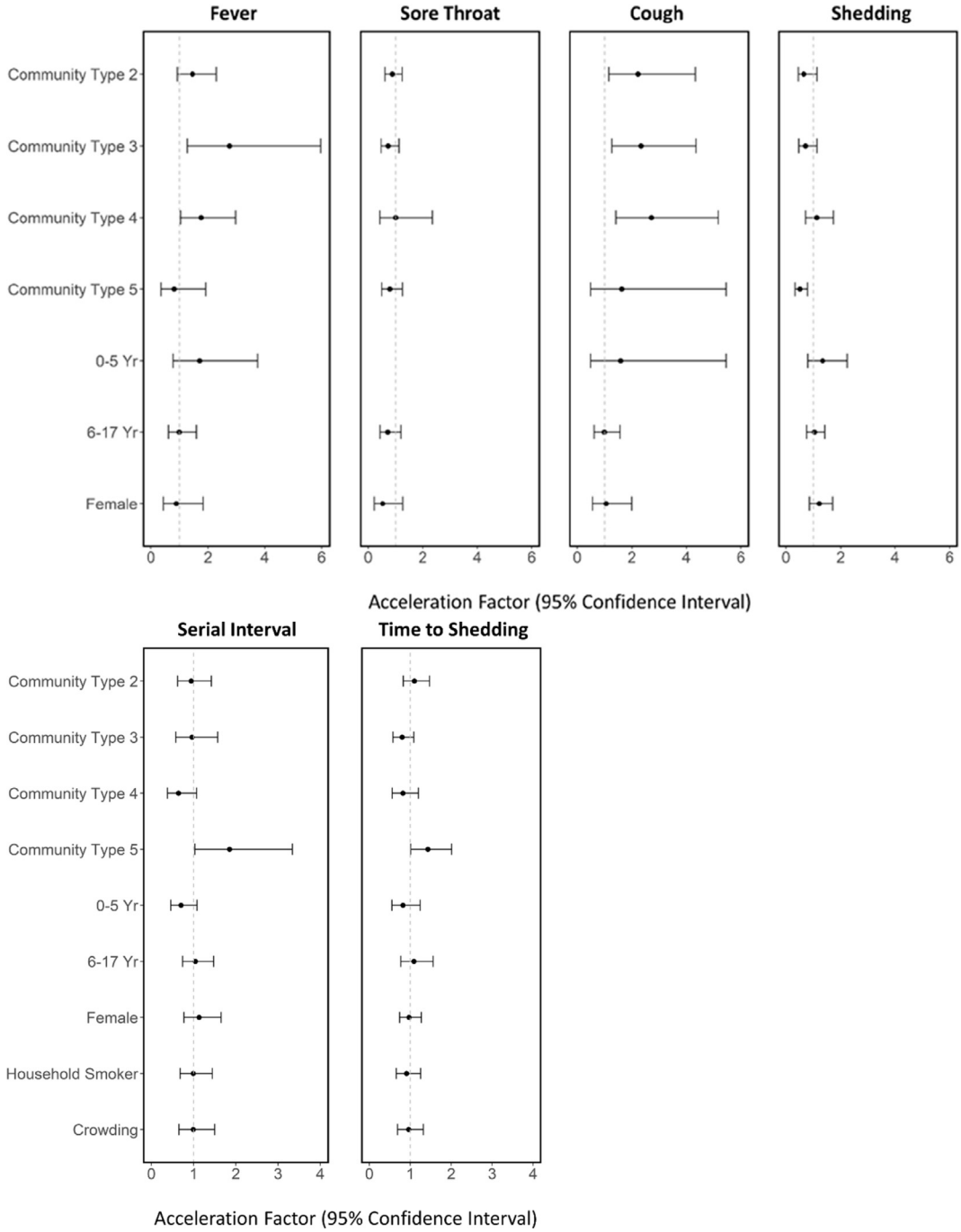

Fig. S5. Accelerated failure time models assessing impact of community types on outcomes of interest among 124 secondary cases from 70 households, Managua, Nicaragua, 2012–2014. Models are not specific to influenza type/subtype. Children 0–5 years of age were removed from the sore throat model as young children are not able to reliably report sore throat.